

## Diffusion in a crystal lattice with nuclear resonant scattering of synchrotron radiation

B. Sepiol

*Institut für Materialphysik der Universität Wien, Strudlhofgasse 4, A-1090 Wien, Austria*

A. Meyer

*Physik-Department E13, Technische Universität München, D-85747 Garching, Germany  
and European Synchrotron Radiation Facility, F-38043 Grenoble, France*

G. Vogl

*Institut für Materialphysik der Universität Wien, Strudlhofgasse 4, A-1090 Wien, Austria*

H. Franz

*Physik-Department E13, Technische Universität München, D-85747 Garching, Germany*

R. Rüffer

*European Synchrotron Radiation Facility, F-38043 Grenoble, France*

(Received 9 October 1997)

We report on a method for probing the elementary diffusion jumps in crystalline lattices on an atomistic scale. The method makes use of synchrotron radiation coherently scattered in the forward direction after nuclear resonant excitation. The decay of forward-scattered radiation is faster (“diffusionally accelerated”) when atoms move on the time scale of the excited-state lifetime because of a loss of coherence. The acceleration of the decay rate differs for different crystal orientations relative to the beam; thus providing information not only about the rates but also about the directions of the diffusion jumps. As a first application we studied the diffusion of  $^{57}\text{Fe}$  in the intermetallic alloy  $\text{Fe}_3\text{Si}$  parallel to the [111] and [113] crystal directions yielding the diffusion mechanism of iron and its diffusion coefficient. From a comparison with conventional quasielastic Mössbauer spectroscopy the advantages of the method are deduced. [S0163-1829(98)07317-2]

### I. INTRODUCTION

After the original proposal by Singwi and Sjölander on how to study diffusion in solids with Mössbauer spectroscopy<sup>1</sup> and the experiments on crystalline solids by Knauer and Mullen<sup>2</sup> that method has been applied with growing success for studying the diffusion mechanism in solids on an atomistic scale.<sup>3</sup> Since the method makes use of quasielastic energy broadening in analogy to quasielastic neutron scattering (QNS) it is called quasielastic Mössbauer spectroscopy (QMS). In the case of QNS, diffusion manifests itself through the energy broadening of the scattered intensity; in the case of QMS, through the change in shape of the nuclear resonance line(s).

Here we present the first full report on a measurement of diffusion *in a single crystal* using the new technique of nuclear resonant scattering of synchrotron radiation<sup>4,5</sup> (SR) (for a review, see Ref. 6). A preliminary letter containing part of the experimental results has been published earlier.<sup>7</sup> Recently nuclear resonant scattering of SR has been applied to the study of dynamics around the glass transition.<sup>8</sup>

The nuclear resonant scattering technique enables studies in the time domain, whereas QMS and QNS studies perform in the energy domain. The general idea using nuclear resonant scattering of synchrotron radiation is that the collective coherent state during the scattering process is destroyed by diffusion, which leads to a faster decay of the scattered intensity in the *forward* direction with respect to an undis-

turbed scattering process. From this “diffusionally accelerated decay,” details on the diffusion process can be derived. We will in the following use the abbreviation NFS for nuclear forward scattering.

The choice of an appropriate system is decisive for a study that is intended to demonstrate the capacities and limitations of this method for investigating diffusion. It should be a well-known material already thoroughly investigated with QMS and the tracer diffusion method. The effects to be expected from diffusion should be of reasonable size under easily manageable experimental conditions.

All these requirements are well fulfilled by the ordered intermetallic alloy  $\text{Fe}_3\text{Si}$  as argued in the following. (a)  $\text{Fe}_3\text{Si}$  crystallizes in a simple structure (cubic  $\text{D0}_3$ , consisting of three iron sites and one silicon site in a primitive cell) and is perfectly ordered up to the melting point ( $T_m \approx 1500$  K). (b) Single crystals of  $\text{Fe}_3\text{Si}$  are stable during high-temperature measurements. They can be grown, oriented, cut and polished up to the required final thickness. (c)  $\text{Fe}_3\text{Si}$  shows extremely fast diffusion of the iron atoms, the fastest of all iron intermetallics with high iron content found up to now. Thus diffusion phenomena can be observed at low temperature (about 900 K), which reduces technical problems. QMS (Refs. 9,10) has proven that Fe atoms which occupy sites on three sublattices (Fig. 1) jump between nearest-neighbor iron sites on different sublattices remaining on each sublattice for different residence times. Tracer diffusion studies<sup>11</sup> have confirmed the diffusivities determined from

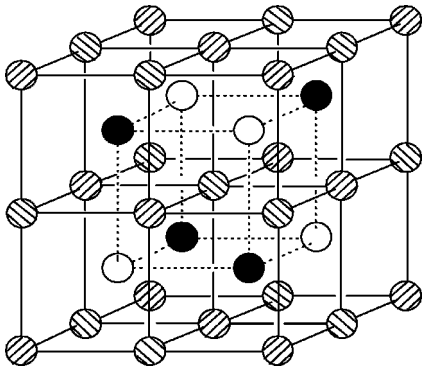


FIG. 1. Elementary cell of the  $D0_3$  structure of  $Fe_3Si$ . The iron atoms occupy the sublattices  $\alpha_1$ ,  $\alpha_2$  (shaded circles), and  $\gamma$  (black circles), the silicon atoms the sublattice  $\beta$  (open circles).

the QMS measurements and extended the determination of diffusivities to a wider temperature range than accessible to QMS.

The aim of this paper is to explore the possibilities of using this new method of studying diffusion, and to study the sensitivity limits of the method. In Sec. II sample preparation and high-temperature measurements with NFS and with QMS are described. In Sec. III we deal first with the method of calculation of NFS spectra in the presence of diffusion. We briefly describe in general form the calculation of the self-correlation function and specify it for the  $D0_3$  structure. We then discuss the particular case of  $Fe_3Si$ . In Sec. IV we interpret NFS spectra on the basis of the theory. In Sec. V we account for the fact that due to the high resolution of the NFS method, with respect to both geometry and time, it is necessary to include relaxation due to jumps of iron atoms between lattice sites with different isomer shifts. Section VI contains conclusions and an outlook.

## II. EXPERIMENT

### A. Sample

Two single crystals of the Fe-Si alloy were grown by the Bridgman technique with the compositions (a) 75.5 at. % Fe, 24.5 at. % Si and (b) 74 at. % Fe, 26 at. % Si, respectively. The ingots were 99.99% iron (Johnson Matthey) and 99.999% silicon (Goodfellow). Sample (a) contained natural iron (concentration of  $^{57}Fe$  2.1 at. %), sample (b) was enriched (5.1 at. %  $^{57}Fe$ ). Preliminary results on sample (a) have already been reported.<sup>7</sup>

For sample (a) two slices of about 10 mm diameter were cut by a wire saw with their surfaces parallel to the (113) plane. After cutting the samples were ground to final thicknesses of 24  $\mu m$  and 15  $\mu m$ , respectively. For sample (b) one slice oriented with its surface parallel to the (335) plane was produced (final thickness 21  $\mu m$ ). The thickness of the slices was constant within about 1  $\mu m$ .

### B. Furnace

The vacuum furnace was produced by CIGNUS (Cracow, Poland). It was originally designed for Mössbauer measurements at temperatures up to about 1100 K. The distance between entrance and exit beryllium windows ( $\phi = 15$  mm) is only 40 mm. These dimensions enable measurements in the

range  $+17^\circ$  to  $-17^\circ$  degrees relative to the furnace axis. Temperature is controlled by a chromel-alumel thermocouple with a relative accuracy of 1 K. The absolute temperature was calibrated via the Curie temperature of the sample (known from a differential scanning calorimeter analysis). For the measurements at the synchrotron and the Mössbauer measurements, as well, the furnace was mounted on a goniometer head permitting a change in the orientation of the samples relative to the direction of the beam.

The samples were encapsulated between two beryllium oxide disks, each one 0.9 mm thick, granting more than 40% transparency for the 14.4 keV radiation. The encapsulation was necessary to avoid inflection of the samples during the measurements at high temperatures.

### C. Measurement of nuclear forward scattering of synchrotron radiation (NFS)

The experiments with nuclear forward scattering of SR were carried out at the nuclear resonance beamline of the ESRF (for details see Ref. 12). The storage ring operated in 16-bunch mode providing short pulses of x rays (duration  $\sim 100$  ps) every 176 ns. The radiation from the undulator source, optimized for the 14.4 keV transition in iron, was filtered by a double Si(111) reflection followed by monochromatization in a nested high resolution monochromator.<sup>12,13</sup> The delayed events, resulting from NFS,<sup>14</sup> were counted by a fast avalanche photo diode (APD) detector.<sup>15,16</sup> Because of overload of the detector from the prompt synchrotron pulse, data taken during the first 20 ns after each pulse have to be discarded.<sup>17</sup> In principle, the duration of this “lost time” is determined by the SR pulse length and the detector resolution ( $\sim 100$  ps FWHM), but due to the detector overload the lost time is considerably longer.

Depending on crystal direction and temperature, the count rates were between 90 (for the [113] crystal direction parallel to the synchrotron beam) and 140 ([111] direction) delayed counts per second at 827 K, and between 3 and 60 delayed counts per second at 967 K. This resulted in measuring times between 5 and 60 min. The constant background of the APD diode was 0.02 cps and could be neglected in the spectra fitting.

### D. Mössbauer measurements

In order to be able to recognize most directly the advantages and possible drawbacks of NFS compared to QMS, we measured with both techniques on identical samples. For the Mössbauer absorption measurements we used a  $^{57}Co$  in Rh source and the same furnace that was afterwards used for the synchrotron experiment. The high-temperature Mössbauer spectra for the sample (a) have been shown in Fig. 2 of Ref. 7. Within the resolution of the Mössbauer method the high-temperature spectra of sample (b) are identical with those of sample (a).

## III. DIFFUSION: PRINCIPLES OF NUCLEAR RESONANT SCATTERING AND MÖSSBAUER SPECTROSCOPY

### A. General outline of the theory of quasielastic methods for studying diffusion

The original theory of Singwi and Sjölander<sup>1</sup> deals with continuous diffusion, whereas Chudley and Elliott shortly

later described jump diffusion on an empty Bravais lattice,<sup>18</sup> i.e., an empty lattice with all sites equivalent. The action of diffusion is contained in what Randl,<sup>19</sup> following the terminology of neutron scattering, calls the intermediate scattering function  $I(\mathbf{Q}, t)$  (named momentum-time correlation function by Smirnov and Kohn<sup>20,21</sup> and marked  $F_s(\mathbf{Q}, t)$  by them).  $I(\mathbf{Q}, t)$  is the Fourier transform from space into momentum of the diffusional part of the space-time self-correlation function  $G(\mathbf{r}, t)$ ,

$$I(\mathbf{Q}, t) = \int d\mathbf{r} \exp(-i\mathbf{Q}\mathbf{r})G(\mathbf{r}, t), \quad (1)$$

where  $\mathbf{Q}$  is the momentum transfer to the interacting radiation. In the case of diffusion  $G(\mathbf{r}, t)$  is the solution of the diffusion equation for the given system.

For diffusion on non-Bravais lattices the intermediate scattering function can be written in the following way:<sup>22,19</sup>

$$I(\mathbf{Q}, t) = \sum_p w_p(\mathbf{Q}) \exp[\Gamma_p(\mathbf{Q})t/2\hbar], \quad (2)$$

where  $\Gamma_p(\mathbf{Q})/2\hbar$  is the  $p$ th *negative* eigenvalue of the *jump matrix*  $\mathbf{A}$  and

$$w_p(\mathbf{Q}) = \left| \sum_i \sqrt{c_i} b_i^p \right|^2. \quad (3)$$

$w_p(\mathbf{Q})$  is the weight of the component in the measured spectra corresponding to the  $p$ th eigenvalue, with  $c_i$  the probability of finding the atom on the  $i$ th sublattice and  $b_i^p$  the  $i$ th component of the  $p$ th eigenvector of the jump matrix. The elements of the jump matrix  $\mathbf{A}$  are given by

$$A_{ij} = \frac{1}{n_{ji} \tau_{ji}^k} \sum_k \exp(-i\mathbf{Q}\mathbf{l}_{ij}^k) - \delta_{ij} \sum_j \frac{1}{\tau_{ij}}. \quad (4)$$

Here each site of the  $i$ th sublattice is surrounded by  $n_{ij}$  sites of the  $j$ th sublattice with the  $k$ th site at a vector distance  $\mathbf{l}_{ij}^k$ .  $\tau_{ij}^{-1}$  is defined as the jump rate from a site of symmetry  $i$  to any nearest-neighbor site of symmetry  $j$ . Generally, for a nonequal occupation of different sublattices due to, e.g., lattice disorder, the matrix  $\mathbf{A}$  is not Hermitian and must be transformed by a similarity transformation into Hermitian form.<sup>19</sup> The elements of the jump matrix  $\mathbf{A}$  specify the various allowed jumps for the diffusing atom and the accompanying jump rates.

The momentum-energy correlation function (called the universal resonance function by Smirnov and Kohn<sup>20,21</sup>)  $\varphi(\mathbf{Q}, \omega)$  is calculated by the Laplace transformation,

$$\varphi(\mathbf{Q}, \omega) = \frac{\Gamma_0}{2\hbar} \int_0^{+\infty} dt \exp(i\omega t - \Gamma_0 t/2\hbar) I(\mathbf{Q}, t), \quad (5)$$

and further on from Eq. (2),

$$\varphi(\mathbf{Q}, \omega) = i \sum_p \frac{w_p(\mathbf{Q}) \Gamma_0/2\hbar}{\omega + i(\Gamma_0 - \Gamma_p(\mathbf{Q}))/2\hbar}, \quad (6)$$

where for QMS and NFS,  $\Gamma_0$  is the energy width of the excited nuclear level and  $-\Gamma_p(\mathbf{Q})$  is the energy width (FWHM) caused by diffusion leading for QMS to ‘‘diffusional line broadening.’’

$\varphi(\mathbf{Q}, \omega)$  mirrors all dynamical effects on QMS, QNS, and NFS spectra: In QMS the real part of  $\varphi(\mathbf{Q}, \omega)$  called  $S(\mathbf{Q}, \omega)$  in earlier papers<sup>19</sup> is the essential factor of the absorption cross section and of the emission probability and in QNS of the scattering cross section.

### B. Diffusion in Fe<sub>3</sub>Si

In the present paper we study diffusion in an ordered alloy, namely Fe<sub>3</sub>Si, which crystallizes in cubic D0<sub>3</sub> structure (Fig. 1). The D0<sub>3</sub> superlattice is built up of four interpenetrating fcc sublattices with three of them (two named  $\alpha$ , also called  $A$  and  $C$  in the literature and one  $\gamma$  or  $B$ ) occupied by iron atoms and the fourth ( $\beta$  or  $D$ ) by silicon. The  $\alpha$  sublattice can be divided into two parts with different symmetry of  $\gamma$  and  $\beta$  nearest neighbors (NN’s). Iron atoms on  $\alpha$ -sublattice sites have four iron NN’s on  $\gamma$ -sublattice sites, whereas iron atoms on  $\gamma$ -sublattice sites have eight iron NN’s on  $\alpha$  sublattice sites. In earlier Mössbauer work<sup>9</sup> it has been proven that a simple diffusion model with NN jumps of iron atoms between  $\alpha$  and  $\gamma$  iron sublattice sites describes diffusion in the stoichiometric composition. The jumps of silicon atoms are much slower and decoupled from the iron jumps.<sup>11</sup>

For a stoichiometric D0<sub>3</sub> structure the jump matrix  $\mathbf{A}$  Eq. (4) has the following form:<sup>9</sup>

$$\mathbf{A} = \frac{1}{\tau_{\alpha\gamma}} \begin{pmatrix} -2 & E & E^* \\ E^* & -1 & 0 \\ E & 0 & -1 \end{pmatrix}. \quad (7)$$

Here  $\tau_{\alpha\gamma}^{-1}$  is the jump rate of the iron atom from a site on one  $\alpha$  sublattice into a vacancy on a distinct NN site on the  $\gamma$  sublattice and vice versa and  $E$  is a function of the structure of the *jump lattice*,

$$E = \cos(Q_x d) \cos(Q_y d) \cos(Q_z d) + i \sin(Q_x d) \sin(Q_y d) \sin(Q_z d), \quad (8)$$

with  $Q_x$ ,  $Q_y$ , and  $Q_z$  the components of the vector of transferred momentum ( $|\mathbf{Q}| = 7.3 \text{ \AA}^{-1}$  for <sup>57</sup>Fe) and  $d = a/4$ , where  $a$  is the Fe<sub>3</sub>Si lattice constant ( $a = 5.655 \text{ \AA}$  at room temperature and  $5.726 \text{ \AA}$  at 967 K). Because we assumed only NN iron jumps the matrix elements  $A_{23}$  and  $A_{32}$  corresponding to jumps between both  $\alpha$  sublattices are zero. The matrix says that in general there will be three components in the spectra with three different eigenvalues  $\Gamma_p/2\hbar$  (for QMS corresponding to three diffusional broadened lines) and corresponding weights.<sup>9</sup>

With  $\mathbf{Q}$  parallel to special crystal directions, the number of components can be less than three: there are only two components when  $\mathbf{Q}$  is parallel to the [113] crystal direction and even only one for the [111] direction.

## IV. DIFFUSION: EXPERIMENTAL RESULTS AND THEIR INTERPRETATION

As can be derived from what has been said before, in QMS diffusion leads to a simple broadening of one or more Lorentzian-shaped lines.<sup>19</sup> The above-described way of determining diffusional line broadening was applied in Refs. 9, 10, and 19 to QMS and QNS.

On the basis of the same theory, by calculating the Fourier integral over  $\varphi(\mathbf{Q}, \omega)$ , Smirnov and Kohn<sup>20,21</sup> have determined the time dependence of the amplitude of the electric field  $E(t, z)$  for NFS transmitted through the sample of thickness  $z$ . Physically speaking that means considering the interference of all forward scattered components,

$$E(t, z) = E_0(z) \int_{-\infty}^{+\infty} \frac{d\omega}{2\pi} \exp(-i\omega t) \exp[-\frac{1}{2}L\varphi(\mathbf{Q}, \omega)], \quad (9)$$

where  $L = \sigma_0 f_{\text{LM}} n \chi z$  is the effective sample thickness with  $\sigma_0$  the nuclear absorption cross section ( $2.56 \times 10^{-22} \text{ m}^2$ ),  $f_{\text{LM}}$  the Lamb-Mössbauer factor,  $n$  the number of iron atoms per unit volume, and  $\chi$  the  $^{57}\text{Fe}$  isotope abundance. The function  $E_0(z)$  is determined by the intensity of the SR within the frequency band of the monochromator system reduced by electronic absorption in the sample. The intensity of NFS is the square modulus of  $E(t, z)$ .

The essential result of the calculation is the following: When the time between diffusive jumps becomes comparable to or even shorter than the natural lifetime of the nucleus ( $\tau_0 = 141 \text{ ns}$ ), the coherence will be destroyed. This will lead to an accelerated decay rate of the coherently forward scattered intensity.

We now turn to our special case: diffusion in  $\text{Fe}_3\text{Si}$ . In a thin target, the initial time response of the diffusively accelerated decay in NFS is exponential. As has been argued in Ref. 7 for the explanation of NFS spectra one (for Bravais lattices) or several exponential decays (for non-Bravais lattices) are expected, with their number equal to the number of the corresponding absorption lines in Mössbauer spectroscopy.

This approximation was applied in the earlier short communication<sup>7</sup> on diffusion in  $\text{Fe}_3\text{Si}$  studied by NFS. There the time-dependent spectra measured in the [113] direction were fitted with a sum of two exponentials: one decay with natural lifetime corresponding to the unbroadened Mössbauer line with natural linewidth  $\Gamma_0$ , the other faster decay (“diffusionally accelerated”) with slope and relative contribution determined from a free fit corresponding to the broad line in Ref. 9. The validity of this approximation, called also a kinematical approximation for a thin sample was confirmed in the Ref. 21. Each line in the Mössbauer spectrum gives actually rise to one exponential decay of intensity, but as NFS is a coherent scattering method, interference terms between the different resonances contribute to the total intensity.

As has already shortly been reported in Ref. 7, the fits made use of the known values of sample thickness  $z$  and Debye temperature of  $\text{Fe}_3\text{Si}$ ,  $\theta_D = 369 \text{ K}$ , known from Mössbauer and phonon measurements,<sup>23</sup> and yielded consistency with the atomistic diffusion model put up from QMS.<sup>9</sup> From  $\Gamma_p$  the iron diffusivity was calculated.

Sample (b) was measured in two orientations, namely, (i) with the [113] and (ii) the [111] crystal directions parallel to the synchrotron beam (one measurement was performed in the [335] direction). From the Debye temperature, sample thickness  $z = 21(1) \mu\text{m}$  and  $^{57}\text{Fe}$  isotope enrichment  $\chi$

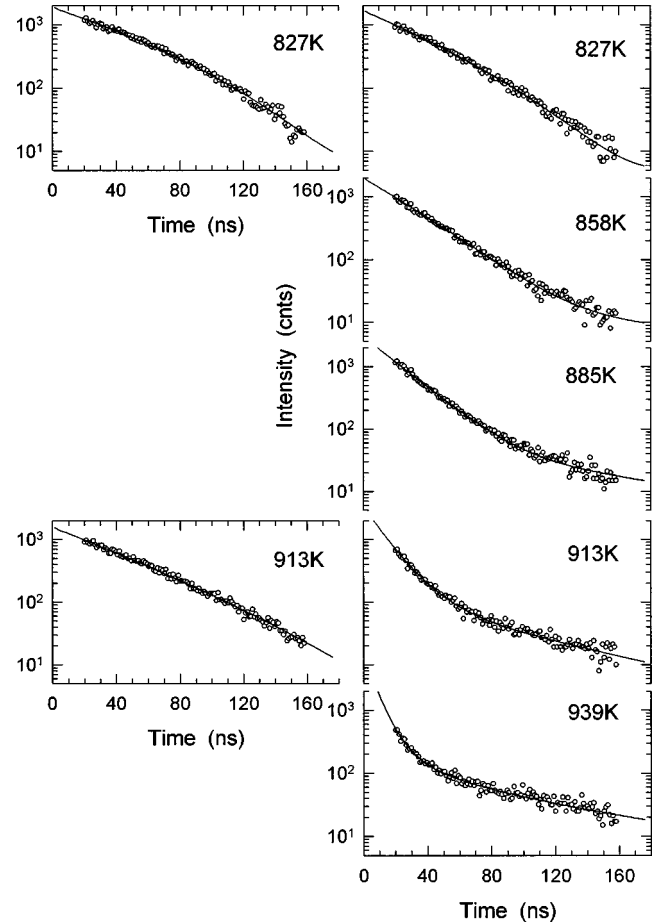


FIG. 2. Nuclear forward scattering of SR from the  $\text{Fe}_3\text{Si}$  sample (b) with the synchrotron beam parallel to the directions [111] (left) and [113] (right). The full lines are fits according to the theory of Sec. V. Note the nearly exponential decay along [111] and the more complicated decay along [113] at elevated temperatures.

$= 5.1\%$ , the effective sample thickness can be calculated to lie between 8.0 at 827 K and 7.0 at 967 K with about 10% error.

Figure 2 shows time spectra of forward-scattered intensity as a function of time after the SR pulse for both sample orientations and at two and five different temperatures, respectively. Figure 3 shows NFS spectra with the beam parallel to three different crystal directions all at 967 K (this was the highest measuring temperature). The strong dependence of the spectrum shape both on temperature and on the direction is clearly visible. The lines in Figs. 2 and 3 are fitted with the complete theory described further down in Sec. V.

We eventually, however, ran into a problem with the calculations based on Eqs. (6) and (9). As can be seen from Fig. 4, where we show NFS spectra in the [113] direction, at sufficiently high temperature (shown here is 939 K) the spectrum can be well described with weights  $w_p = 0.9$  and 0.1 [Eq. (3)] for the fast and the slow components in agreement with a model of jumps between the  $\alpha$ - and  $\gamma$ -Fe sites.<sup>24</sup> For lower temperatures, however, shown here is 885 K, it is evident that the model described above does not fit (dashed line). Fitting weights  $w_p$  and different isomer-shift values for both components [ $\omega - \omega_p$  in Eq. (6)] provides much better agreement with experiment (full curve in Fig. 4). The reason of the effective change in weight [ $w_p(\mathbf{Q})$  of the fast compo-

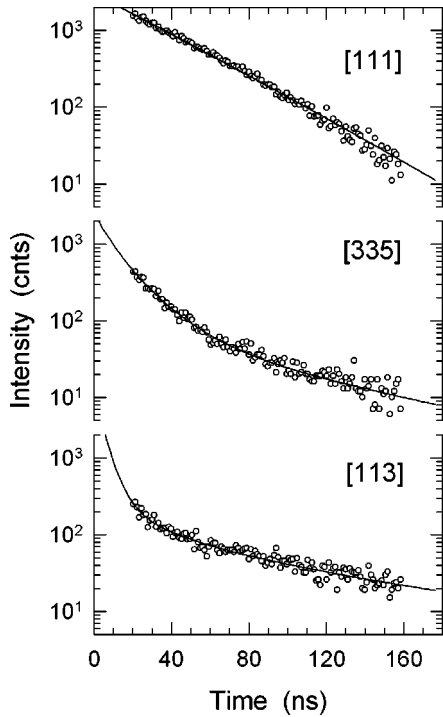


FIG. 3. NFS spectra of  $\text{Fe}_3\text{Si}$  sample (b) with the synchrotron beam along three different crystal directions taken at 967 K. Lines are fits according to the theory of Sec. V.

ment decreases with decreasing temperature to about 0.7 at 885 K] must be sought in incomplete description of the experimental results by the model used up to now. We seek the reason for that deficiency in the following: what has been neglected is the relaxation of isomer shifts of various components due to the mobility of the atoms. It is appealing that the measured temperature dependence of weights is a relaxational effect. This effect was suggested<sup>25</sup> but not evident

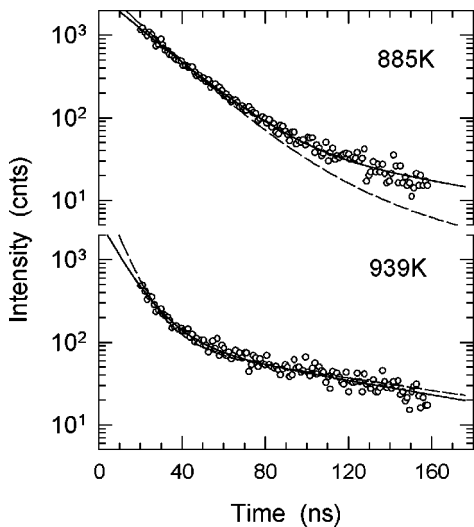


FIG. 4. NFS spectra of  $\text{Fe}_3\text{Si}$  sample (b) with the synchrotron beam along [113] direction taken at 885 and 939 K. Dashed curves: fit with model of Secs. III and IV, without accounting for relaxation and without the difference in isomer shift between the component corresponding to the unbroadened resonance and the faster (diffusionally accelerated) component. Full curves: isomer shift difference and contributions are fitted.

from QMS with its poorer effective energy resolution due to the poor angular resolution of Mössbauer spectroscopy. In the following we seek to include the effects of relaxation of hyperfine interactions into our model.

## V. FLUCTUATING HYPERFINE INTERACTIONS AND DIFFUSION

Different iron sites in intermetallic alloys feel different hyperfine interactions, resulting from the difference in their atomic neighborhood. In general this leads to an isomer shift due to Fe atoms at different sites or causes quadrupole splitting due to a noncubic symmetry of the neighborhood or leads to magnetic splitting in a magnetic neighborhood. In the present case (cubic, paramagnetic in the relevant temperature range) only an isomer shift between the components from the  $\alpha$  and  $\gamma$  sites of Fe atoms can appear.

At low temperatures where diffusion is very slow, in fact two lines appear in the Mössbauer spectra with proportion being 2:1 originating from the occupation of the  $\alpha$  and  $\gamma$  sublattices by  $^{57}\text{Fe}$  atoms independent of crystal orientation.

At very high temperatures where only diffusion defines the spectrum shape, and relaxation effects are veiled by the large width of the lines, the diffusion theory of Sec. III suffices, the weights being given by the solution of Eq. (3) with the jump matrix Eq. (7). In particular, for the spectra in [113] direction the weights of broad and narrow line are 0.9 and 0.1, respectively<sup>9,21</sup> (see Fig. 4, 939 K).

We now turn to the *intermediate temperature region*. Here the hyperfine components start to fluctuate, if the atoms jump between lattice sites during the lifetime of the excited nuclear state, but this fluctuation is still not veiled by the diffusional linewidth as is the case for very high temperatures.

The theory of the combined effects of diffusion and fluctuating hyperfine interaction has been developed by Dattagupta<sup>26</sup> and Dattagupta and Schroeder<sup>27</sup> who adapted the Blume<sup>28</sup> approach for incorporating diffusion effects to QMS. They get

$$\varphi(\mathbf{Q}, \omega) = \frac{\Gamma_0}{2\hbar i} \sum_{k,m} \left( k \left| \left[ \left( i\omega + \frac{\Gamma_0}{2\hbar} \right) \times \mathbf{1} - \mathbf{A} \right]^{-1} \right| m \right) c_m, \quad (10)$$

where  $\mathbf{1}$  is a unit matrix, the term in parentheses is the matrix element  $(k, m)$  and  $k$  and  $m$  are sublattice indices. This method demands a matrix inversion but offers the possibility to introduce effects of the relaxation of hyperfine interactions. Dattagupta and Schroeder were interested in QMS and QNS and therefore calculated only the real part of  $\varphi(\mathbf{Q}, \omega)$ , which is essentially the absorption probability and the scattering cross section.

The Dattagupta-Schroeder approach was developed in principle to include the effect of vacancies near the Mössbauer atom. In diffusion in the intermetallic phase  $\text{Fe}_3\text{Si}$  we neglect the influence of vacancies due to the negligibly low values<sup>29</sup> of vacancy-induced hyperfine interactions in this alloy. We rather consider here only one type of hyperfine interactions, namely, the monopole interaction responsible for the isomer shift differences due to different distributions of Fe and Si atoms in the neighborhood of the  $^{57}\text{Fe}$  atoms, i.e.,

TABLE I. Sample thickness  $L$ , jump rate  $\tau_{\alpha\gamma}^{-1}$  and diffusivity  $D$  as a function of temperature and crystal orientation for sample (b). Data as in Fig. 5. Values without errors were kept fixed in the fit.

T (K)	Direction	$L$	$\tau_{\alpha\gamma}^{-1} \times 10^6$ (s $^{-1}$ )	$D$ (m $^2$ s $^{-1}$ )
827	[113]	7.1(4)	0.9(3)	$1.2(4) \times 10^{-14}$
858	[113]	6.2(4)	3.8(5)	$5.1(7) \times 10^{-14}$
885	[113]	6.2(4)	6.7(3)	$9.1(4) \times 10^{-14}$
913	[113]	6.7	13.8(8)	$1.9(1) \times 10^{-13}$
939	[113]	6.3	31(3)	$4.2(4) \times 10^{-13}$
967	[113]	6.0	48(5)	$6.6(7) \times 10^{-13}$
967	[335]	6.0	40(5)	$5.4(7) \times 10^{-13}$
827	[111]	6.9(4)	0.3(3)	$0.4(4) \times 10^{-14}$
913	[111]	6.7(4)	13.8	$1.9 \times 10^{-13}$
967	[111]	6.0	50(5)	$6.7(7) \times 10^{-13}$

on  $\alpha$  and  $\gamma$  sites. This is done, following Ref. 27 by adding the isomer-shift matrix  $\mathbf{V}$  to Eq. (10).

$$\varphi(\mathbf{Q}, \omega) = \frac{\Gamma_0}{2\hbar} \sum_{k,m} \left( k \left[ \left( i\omega + \frac{\Gamma_0}{2\hbar} \right) \times \mathbf{1} - \mathbf{A} - i\mathbf{V} \right]^{-1} \right) \Big|_m \Big) c_m. \quad (11)$$

The isomer-shift matrix can be added as a constant, since it is independent of the nuclear variables of the excited and ground states of the Mössbauer nucleus. For Fe $_3$ Si it has the following form:

$$\mathbf{V} = \begin{pmatrix} \Delta\delta & 0 & 0 \\ 0 & 0 & 0 \\ 0 & 0 & 0 \end{pmatrix}, \quad (12)$$

where  $\Delta\delta$  is the isomer shift difference between  $\alpha$  and  $\gamma$  iron sites (absolute values of isomer shifts are not measured in NFS). The value of  $\Delta\delta$  is known from the RT-Mössbauer measurements and is practically temperature independent [0.16(1) mm s $^{-1}$ ]. By substituting Eq. (12) into Eq. (11) and the result into Eq. (9) the shape of the forward-scattered intensity for diffusion in Fe $_3$ Si is calculated.

To fit the spectra the numerical procedures of matrix inversion and fast Fourier transformation (FFT) from the NAG-Fortran Library Routine Document were applied. The number of fitted parameters was reduced from five to three compared to the fit with two Lorentzian lines. The only fitted parameters for diffusion in the D0 $_3$  lattice are the scattering intensity at time zero (which is in fact a trivial parameter proportional to the measuring time and the synchrotron current only), the sample thickness  $L$  and the jump rate, the latter being the only diffusional parameter. The isomer-shift difference between iron positions on  $\alpha$  and  $\gamma$  sublattices was held constant at 0.16 mm s $^{-1}$ .

As to be seen from Fig. 4, T=885 K, the full curve which takes into account relaxation, gives a much better description of the continuous change of the time spectrum than the dashed curve, which does not account for relaxation.<sup>30</sup> All solid lines in Figs. 2 and 3 were fitted with the above-described method, too. The fitted parameters are listed in Table I. The effective thicknesses of the sample are in good agreement with the values approximated from the measured

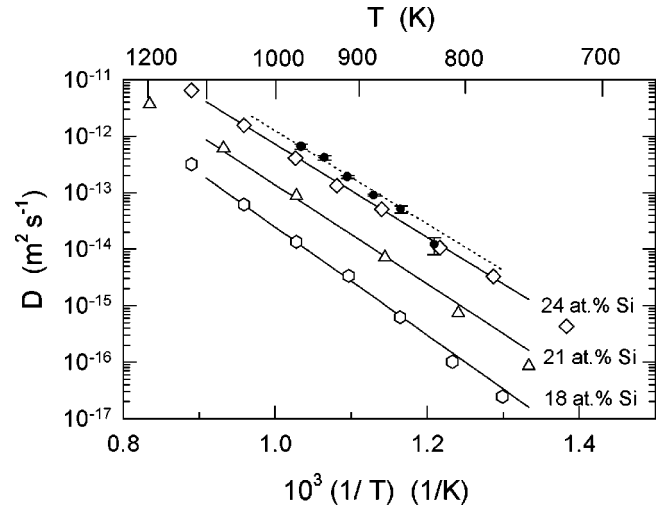


FIG. 5. Diffusivities of Fe in Fe $_3$ Si. Full circles present our NFS result for sample (b), 74 at. % Fe, 26 at. % Si. Diamonds, triangles, and hexagons, data from tracer diffusion studies by Gude and Mehrer, Ref. 11.

thickness  $z$  taking into account its roughly estimated character. Note that due to the method of the single-crystal foil preparation (grinding), the thickness of the foil is sufficiently constant and to use a thickness distribution was not necessary.

For the sake of comparison with the result of other diffusion studies it is useful to calculate the diffusivities from the diffusional acceleration of the intensity decay. Diffusion jumps with jump rates  $\tau_{ij}^{-1}$  in intermetallic compounds between  $i$ th and  $j$ th sublattices with distance vectors  $\mathbf{l}_{ij}$  contribute as partial diffusivities to the diffusion coefficient<sup>31</sup>

$$D = \frac{1}{6} \sum_{i,j} \mathbf{l}_{ij}^2 \tau_{ij}^{-1} c_i, \quad (13)$$

where  $c_i$  are sublattice occupations. Taking into account that we have only one jump rate  $\tau_{\alpha\gamma}^{-1}$  (due to the equal sublattice occupations) and with  $|\mathbf{l}_{ij}| = a\sqrt{3}/4$ , Eq. (13) can be simplified to the form  $D = (1/24)a^2\tau_{\alpha\gamma}^{-1}$ . The resulting diffusivities are given in Fig. 5 and Table I. They are in good agreement with data from literature [QMS (Ref. 32) and tracer diffusivity<sup>11</sup>] showing the reliability of the new NFS method for studying diffusion.

In retrospect we have to admit that the influence of different isomer shifts from different iron sites and their relaxation could have been recognized in Mössbauer spectra as well, again at moderate temperature. There line smearing appeared around 900 K.<sup>25</sup> At high temperatures the increasing diffusional broadening again veils the small differences in the isomer shift of the Mössbauer lines. The reason why relaxation effects are more evident in NFS spectra than in QMS spectra is twofold: (a) QMS spectra are the result of a convolution with the geometrical resolution (the divergence of  $\gamma$  rays for receiving reasonable statistics in reasonable time was about 7 $^\circ$ ), which forbids an experimental resolution of the small energy shifts, as, e.g., small isomer shifts and, in particular, their change through relaxation. The synchrotron beam, in contrast, has nearly negligible divergence, so that the problem with the geometrical resolution is absent.

(b) In QMS the Mössbauer source adds its linewidth to the spectrum, which is not the case for time-resolved NFS with synchrotron radiation.

## VI. CONCLUSIONS AND OUTLOOK

In conclusion we state that it is possible to follow diffusion in the time domain by observing the diffusional acceleration of the decay rate of nuclear forward scattering (NFS) of SR, in analogy to conventional quasielastic Mössbauer spectroscopy (QMS) or quasielastic neutron scattering (QNS), both in the energy domain. The conclusions from the Mössbauer measurements on the jump mechanism are fully confirmed: the jumps are between Fe NN sites on  $\alpha$  and  $\gamma$  sublattices.

NFS spectra can be fitted in a consistent way if one uses a full relaxational-matrix formalism. Uncorrelated jumps between NN sites are sufficient to fit the spectra. Attempts to include correlations between jumps based on the Monte Carlo simulations did not improve the fit quality. The problem of correlation between diffusion jumps in a  $\text{D}_0_3$  lattice has been studied through calculations by Szabó<sup>33</sup> with the result that assuming only nearest neighbor jumps provides sufficient agreement with experimental results.

There are a few definite advantages of the NFS method. (a) Diffusion investigations are orders of magnitude faster than with classical Mössbauer spectroscopy QMS. This permits fast measurements even of samples that stand the high temperatures only for short time. Even shorter measuring times will be possible by the help of an integral method where all delayed counts irrespective of the delay time are counted as a function of the crystal orientation.<sup>34</sup> (b) The highly brilliant synchrotron beam with a size of less than  $1 \text{ mm}^2$  at the sample position and a divergence in the  $\mu\text{rad}$  range permits measurements with considerably reduced “smearing” of the crystal orientation. (c) The narrow beam will enable diffusion investigations in tiny crystals and recrystallized foils.

## ACKNOWLEDGEMENTS

The authors appreciate the most valuable discussions with V. G. Kohn and G. V. Smirnov and the continuous exchange of ideas with W. Petry. They thank A. Q. R. Baron for help with the APD detector and A. I. Chumakov for advice with the experiments. This work was supported by grants from the Austrian FWF (Project No. S5601) and from the German BMBF (Project No. 05 643WOB).

- 
- <sup>1</sup>K. S. Singwi and A. Sjölander, Phys. Rev. **119**, 863 (1960); **120**, 1093 (1960).
- <sup>2</sup>R. C. Knauer and J. G. Mullen, Phys. Rev. **174**, 711 (1968).
- <sup>3</sup>G. Vogl, *Diffusion Studies by Mössbauer Spectroscopy*, in Mössbauer Spectroscopy Applied to Magnetism and Materials Science, Vol. 2, edited by G. J. Long and F. Grandjean (Plenum Press, New York, 1996), p. 85; B. Sepiol, Defect Diffus. Forum **125-126**, 1 (1995).
- <sup>4</sup>E. Gerdau, R. Ruffer, H. Winkler, W. Tolksdorf, C. P. Klages, and J. P. Hannon, Phys. Rev. Lett. **54**, 835 (1985).
- <sup>5</sup>See e.g., E. Gerdau and U. van Bürck, in *Resonant Anomalous X-Ray Scattering. Theory and Applications*, edited by G. Materlik, C. J. Sparks, and K. Fischer (Elsevier, Amsterdam, 1994), p. 589.
- <sup>6</sup>G. V. Smirnov, Hyperfine Interact. **97/98**, 551 (1996).
- <sup>7</sup>B. Sepiol, A. Meyer, G. Vogl, R. Ruffer, A. I. Chumakov, and A. Q. R. Baron, Phys. Rev. Lett. **76**, 3220 (1996).
- <sup>8</sup>A. Meyer, H. Franz, J. Wuttke, W. Petry, N. Wiele, R. Ruffer, and C. Hübsch, Z. Phys. B **103**, 479 (1997).
- <sup>9</sup>B. Sepiol and G. Vogl, Phys. Rev. Lett. **71**, 731 (1993).
- <sup>10</sup>B. Sepiol and G. Vogl, Hyperfine Interact. **95**, 149 (1995).
- <sup>11</sup>A. Gude and H. Mehrer, Philos. Mag. A **76**, 1 (1997).
- <sup>12</sup>R. Ruffer and A. I. Chumakov, Hyperfine Interact. **97-98**, 509 (1996).
- <sup>13</sup>T. Ishikawa, Y. Yoda, K. Izumi, C. K. Suzuki, X. W. Zhang, M. Ando, and S. Kikuta, Rev. Sci. Instrum. **63**, 1015 (1992).
- <sup>14</sup>J. B. Hastings, D. P. Siddons, U. van Bürck, R. Hollatz, and U. Bergmann, Phys. Rev. Lett. **66**, 770 (1991).
- <sup>15</sup>S. Kishimoto, Rev. Sci. Instrum. **63**, 824 (1992).
- <sup>16</sup>A. Q. R. Baron and S. L. Ruby, Nucl. Instrum. Methods Phys. Res. A **343**, 517 (1994); A. Q. R. Baron, *ibid.* **352**, 665 (1995).
- <sup>17</sup>In our first measurements this time had been 30 ns; in the meantime the time response of the APD detector has been improved.
- <sup>18</sup>C. T. Chudley and R. J. Elliott, Proc. Phys. Soc. London **77**, 353 (1961).
- <sup>19</sup>O. G. Randl, B. Sepiol, G. Vogl, R. Feldwisch, and K. Schroeder, Phys. Rev. B **49**, 8768 (1994).
- <sup>20</sup>G. V. Smirnov and V. G. Kohn, Phys. Rev. B **52**, 3356 (1995).
- <sup>21</sup>V. G. Kohn and G. V. Smirnov, Phys. Rev. B **57**, 5788 (1998).
- <sup>22</sup>J. M. Rowe, K. Sköld, H. E. Flotow, and J. J. Rush, J. Phys. Chem. Solids **32**, 41 (1971).
- <sup>23</sup>O. G. Randl, G. Vogl, W. Petry, B. Hennion, B. Sepiol, and K. Nembach, J. Phys.: Condens. Matter **7**, 5983 (1995).
- <sup>24</sup>The weights of the components for all angles between [001] and [110] crystal directions are plotted in Fig. 2 of Ref. 9.
- <sup>25</sup>J. Pelloth, B. Sepiol, and G. Vogl (unpublished).
- <sup>26</sup>S. Dattagupta, Phys. Rev. B **12**, 47 (1975).
- <sup>27</sup>S. Dattagupta and K. Schroeder, Phys. Rev. B **35**, 1525 (1987).
- <sup>28</sup>M. Blume, Phys. Rev. **174**, 351 (1968).
- <sup>29</sup>G. Rixecker, P. Schaaf, and U. Gonser, Phys. Status Solidi A **139**, 309 (1993).
- <sup>30</sup>A small difference between RT-Mössbauer spectra (not shown here) of sample (a), 75.5 at. % Fe and sample (b), 74 at. % Fe can be explained by the occurrence of Fe sites with different numbers of silicon atoms in the neighbor shells. This might be attributed to Fe atoms in Fe-rich antiphase boundaries (APB's), as found by G. Rixecker, P. Schaaf, and U. Gonser, Phys. Status Solidi A **151**, 291 (1995) and by K. Hilfrich, W. Kölker, W. Petry, O. Schärpf, and E. Nembach, Z. Metallkd. **84**, 255 (1993). With a small contribution of slower diffusing atoms, i.e., atom's in APB's, a further improvement of the fits is achieved.
- <sup>31</sup>K. W. Kehr, D. Richter, and R. H. Swedensen, J. Phys. F **8**, 433 (1978).
- <sup>32</sup>A. Gude, B. Sepiol, G. Vogl, and H. Mehrer, Defect Diffus. Forum **143-147**, 351 (1997).
- <sup>33</sup>I. A. Szabó, Defect Diffus. Forum **143-147**, 327 (1997).
- <sup>34</sup>A. Meyer, B. Sepiol, G. Vogl, H. Franz, and R. Ruffer, Phys. Rev. B (to be published).